Research Square

Preprints are preliminary reports that have not undergone peer review.
They should not be considered conclusive, used to inform clinical practice,
or referenced by the media as validated information.

Treatment Dependent Response Modeling Using Morphologic and Qualitative Features from Perfusion and Contrast-Enhanced Susceptibility Imaging in Undifferentiated Pleomorphic Sarcoma: A Comparison of Radiation Alone Versus Consecutive Chemotherapy and Radiation

Raul F. Valenzuela

rfvalenzuela@mdanderson.org

The University of Texas MD Anderson Cancer Center

Elvis Duran-Sierra

The University of Texas MD Anderson Cancer Center

Ahsan Farooqi

The University of Texas MD Anderson Cancer Center

Alexander J. Lazar

The University of Texas MD Anderson Cancer Center

Mathew Antony

The University of Texas MD Anderson Cancer Center

Keila E. Torres

The University of Texas MD Anderson Cancer Center

Jossue Espinoza-Figueroa

The University of Texas MD Anderson Cancer Center

Behrang Amini

The University of Texas MD Anderson Cancer Center

Dejka M. Araujo

The University of Texas MD Anderson Cancer Center

Sam Lo

The University of Texas MD Anderson Cancer Center

John E. Madewell

The University of Texas MD Anderson Cancer Center

William A. Murphy

The University of Texas MD Anderson Cancer Center

Jingfei Ma

The University of Texas MD Anderson Cancer Center
Ken-Pin Hwang
The University of Texas MD Anderson Cancer Center
R. Jason Stafford
The University of Texas MD Anderson Cancer Center
Chengyue Wu
The University of Texas MD Anderson Cancer Center
David Wells
The University of Texas MD Anderson Cancer Center
Nisha Yadav
The University of Texas MD Anderson Cancer Center
Ali Askari
The University of Texas MD Anderson Cancer Center
Christine Tang
The University of Texas MD Anderson Cancer Center
Pia V. Valenzuela
The University of Texas MD Anderson Cancer Center
Corinne Lo
The University of Texas MD Anderson Cancer Center
Colleen M. Costelloe
The University of Texas MD Anderson Cancer Center

Research Article

Keywords: Soft tissue sarcoma (STS), Undifferentiated pleomorphic sarcoma (UPS), Pathology-assessed treatment effect (PATE), Multiparametric MRI, Radiotherapy

Posted Date: August 7th, 2026

DOI: https://doi.org/10.21203/rs.3.rs-10286016/v1

License: This work is licensed under a Creative Commons Attribution 4.0 International License.
Read Full License

Additional Declarations: No competing interests reported.

Abstract

Background: Undifferentiated pleomorphic sarcoma (UPS) is the most common subtype of soft-tissue sarcoma (STS). At our institution, preoperative management typically consists of neoadjuvant chemotherapy plus radiotherapy (CT-RT) or radiotherapy (RT) alone. This study aimed to assess (1) the impact of treatment strategies on therapeutic response, and (2) the utility of multiparametric MRI (mp-MRI), qualitative and morphologic features from contrast-enhanced susceptibility-weighted imaging (CE-SWI) and dynamic contrast-enhanced perfusion-weighted imaging (PWI/DCE), for response evaluation.

Methods: In this IRB-approved retrospective study, 36 UPS patients underwent presurgical mp-MRI between 02/2021 and 03/2025. Unlike our prior STS research, we intentionally excluded clinically unavailable software-based semiquantitative, quantitative, and radiomic analyses, focusing instead on morphologic and qualitative features readily accessible to clinical radiologists. Lesions were morphologically classified by CE-SWI-T2* and PWI/DCE in six patterns, respectively. PWI/DCE Time-intensity curves (TICs) types III—V, characterized by rapid arterial upstroke, were considered “aggressive,” while TIC I–II as non-aggressive. Patients with ≥90% pathology-assessed treatment effect (PATE) on the surgical specimen were designated as responders (n=20), >30 and <90% PATE as partial-responders (n=10), and ≤30% as non-responders (n=6). <90% patients were combined into a single group (partial/non-responders n=16).

Results: Of 36 patients, 23 received CT-RT and 13 received RT alone. The CT-RT group demonstrated a higher responder rate (61% vs. 45%) and a higher mean PATE (81% vs. 66%; P=0.054) than the RT group. Among CT-RT responders, 86% showed a CE-SWI-complete-ring pattern ($P=2.72\times10^{-9}$), 86% a PWI/DCE-capsular-pattern ($P=1.05\times10^{-7}$), and 93% TIC-type-II ($P=1.35\times10^{-5}$). A predictive model combining PWI/DCE-capsular-enhancement, TIC-II, and favorable CE-SWI-patterns (“full blooming” or “complete ring”) achieved excellent performance (AUC=0.98) for distinguishing responders from non-responders, outperforming RECIST (AUC=0.52). In the RT group, all responders demonstrated TIC-II (P=0.014), and a model based solely on TIC-II achieved perfect classification (AUC=1.0).

Conclusion: The CT-RT group shows a non-statistically significant higher proportion of responders and PATE-average than patients receiving RT-alone. MP-MRI-based predictive models using PWI/DCE and CE-SWI morphologic and qualitative clinically available features substantially outperform RECIST in predicting UPS pathology response. While the CT-RT model closely resembled a previously published treatment-agnostic UPS response model, pathology response in RT-alone patients was reliably predicted by the presence of presurgical TIC-II alone, indicating that optimal classification models for distinguishing responders vary by both tumor histology and treatment regimen, underscoring the importance of personalized imaging approaches.

INTRODUCTION

Soft tissue sarcomas (STS) are rare, aggressive malignancies of mesenchymal origin, representing approximately 1–2% of all malignant tumors. Undifferentiated pleomorphic sarcoma (UPS), formerly

known as malignant fibrous histiocytoma, is the most prevalent STS subtype affecting the trunk and extremities, accounting for roughly 10–20% of adult STS cases and occurring predominantly in older people [1]. UPS most often manifests as a painless, rapidly enlarging mass, though clinical presentation may vary with tumor location and size [2]. The prognosis for UPS remains poor, particularly for patients with large or high-grade tumors, positive resection margins, or metastatic (stage IV) disease [3, 4]. Standard management involves wide local excision combined with pre- (neoadjuvant) - or post-operative (adjuvant) radiotherapy, with neoadjuvant chemotherapy indicated in cases of increased metastatic risk, as is often the case in sarcomas larger than 5 cm. Despite these interventions, recurrence rates remain high, highlighting the need for more effective and robust treatment strategies, including flexible regimens based on assessment of therapeutic efficacy while on treatment [2]. In a large, tertiary single-center analysis, 17% of patients with UPS developed local recurrence, while 30% developed metastasis. Lymph node involvement occurred in 13.5% of cases. Among patients with metastatic disease, the lungs were the most affected organ (76.9%) [5].

The standard neoadjuvant radiotherapy (RT) regimen delivers 50 Gy in 25 daily fractions over five weeks [6]. In a prospective, single-arm trial, Guadagnolo et al. evaluated 120 patients with localized STS who received a moderately hypo-fractionated regimen of 42.75 Gy in 15 daily fractions over three weeks. This alternative schedule resulted in rates of major wound complications comparable to those of conventional radiotherapy and was deemed a safe regimen alternative [7]. Long-term follow-up indicates that moderately hypo-fractionated preoperative radiotherapy is both safe and effective for patients with STS [8]. While higher-grade late toxicities occur in a minority of patients, the symptoms decrease over time. Functional outcomes and health-related quality of life also appear to improve over time following combined modality treatment [8].

At our institution, chemotherapy is considered for patients with high-grade tumors larger than 5 cm, as these patients have an elevated risk of developing metastatic disease [7]. Neoadjuvant chemotherapy (CT) offers several potential advantages over an adjuvant chemotherapy approach: it may reduce the extent of surgery required, increase rates of limb salvage, allow early treatment of micro-metastatic disease, and provide an opportunity to assess tumor response [9]. It is currently unknown whether neoadjuvant CT followed by RT (CT-RT) or neoadjuvant RT alone offers the best therapeutic response. Thus, our first study aim is to evaluate the impact of these treatment strategies on therapeutic response.

After treatment, UPS demonstrates areas of necrosis, hyalinization, cytological degeneration, hemorrhage, hemosiderin deposition, and foamy macrophages, reflecting reduced cellularity. These post-treatment changes are essential for determining the percentage of pathology-assessed treatment effect (PATE) [10, 11]. In solid tumors, particularly in several STS, a pathologic complete response (pCR/High-PATE) is considered a favorable prognostic indicator [11]. However, in some STS, and specifically in UPS, the prognostic significance of pCR remains uncertain. Several studies suggest a potential positive correlation between pCR and patient outcomes; achieving pCR has been associated with lower rates of local relapse and improved 5-year disease-specific survival (DSS) and overall survival (OS) [12–14]. For example, Bonvalot et al., in a retrospective multicenter study of 330 patients with

primary nonmetastatic STS of the extremities and trunk wall who received preoperative RT plus chemotherapy or chemoradiotherapy, found that pCR was significantly associated with better distant recurrence-free survival (MFS), local recurrence-free survival (LRFS), disease-free survival (DFS), and 3-year overall survival (OS) [15]. Donahue et al. evaluated neoadjuvant chemotherapy with or without radiation in 55 patients with high-grade retroperitoneal sarcomas and observed that histopathologic response correlated with improved DSS [16]. Wang et al. combined analyses of RTOG trials 0630 and 9514, which assessed clinical outcomes and pathological response in STS patients treated with preoperative RT or neoadjuvant chemoradiotherapy, and found that pCR was associated with improved survival, supporting its use as a prognostic factor in future studies [17].

Imaging biomarkers have been shown to help assess therapeutic response in UPS. Genaro et al., in a cohort of 107 patients with intermediate- or high-grade STS, investigated imaging biomarkers of tumor response by describing changes in imaging and pathology findings after neoadjuvant radiotherapy (nRT).

Conventional MRI characteristics of UPS were evaluated [18]. Approximately 20% of UPS are calcified, while a small proportion demonstrate significant hemorrhage [19, 20]. MRI plays a crucial role in both pre-surgical planning and post-treatment evaluation due to its superior soft tissue contrast. MRI enables detailed assessment of the tumor's anatomical extent, its infiltration into adjacent structures, and the biological changes within the tumor [19]. On conventional MRI, treatment naïve UPS appears as a well-defined, lobulated mass with heterogeneous components. The solid tissue typically shows iso-intensity relative to adjacent muscle on T1-weighted imaging, high signal intensity on T2-weighted imaging, and substantial peripheral enhancement following contrast administration. Areas of hemorrhage exhibit high signal intensity on T1-weighted imaging [19].

Multiparametric MRI (mp-MRI) incorporates advanced imaging modalities—perfusion-weighted imaging with dynamic contrast enhancement (PWI/DCE), Diffusion-weighted imaging and apparent diffusion coefficient (DWI/ADC), and contrast-enhanced susceptibility-weighted imaging (CE-SWI) [21, 22, 23]—to comprehensively assess soft tissue sarcomas (STS). **PWI/DCE**, through rapid serial imaging after contrast administration, enables detailed evaluation of tissue perfusion kinetics and vascularity, using qualitative, semi-quantitative, or quantitative analysis methods. Malignant tumors are characterized by rapid, early enhancement patterns, distinguishing them from benign lesions. **DWI/ADC** utilizes the random movement of water molecules to characterize the cellularity of malignant tumors. **Susceptibility-weighted imaging (SWI)** is a high-resolution, velocity-corrected, three-dimensional gradient-echo sequence that produces images incorporating both magnitude and phase information. The addition of contrast **(CE-SWI)** enhances detection of hemorrhage (T2* susceptibility), necrotic fluid (T2 signal), and viable tumor (T1 shortening) within a single sequence [21, 22, 23]. Recent studies demonstrate that CE-SWI reliably discriminates viable tumors from hemorrhagic or necrotic regions, supporting its emerging role as a biomarker for monitoring therapeutic response [24, 25]. Collectively, these functional MRI sequences have been shown to be valuable for identifying post-treatment histological changes, such as granulation tissue and fibrosis, and for delineating viable from non-viable tumor and non-tumoral tissue [24, 25]. In addition, advanced imaging/mp-MRI has demonstrated

potential to improve assessment of pseudo-progression and biological behavior of STS early after treatment, compared with conventional size-based Response Evaluation Criteria in Solid Tumors (RECIST), World Health Organization (WHO), and volumetric measurements [26–28]. Contrary to several STS publications, DWI/ADC has shown important limitations in assessing UPS response due to interference from T2* hypo-intensity caused by treatment-induced hemorrhage, which lowers ADC values and mimics increased cellularity, leading to spurious and often counterintuitive results [29].

Treatment-naïve UPS typically shows restricted diffusion with low ADC values on DWI/ADC, rapid early enhancement on PWI/DCE, and enhancement of viable tumor on CE-SWI [25, 29–31]. Following successful treatment, UPS shows variable changes in diffusion characteristics, decreased wash-in rates on PWI/DCE, and significant hemorrhage on CE-SWI. However, it is unknown whether optimal imaging biomarkers of response are affected by the treatment strategy.

Recent studies in extremity UPS [25, 29–31], LMS [32], and desmoid fibromatosis [33, 34] have provided initial evidence of the clinical relevance of mp-MRI for imaging and quantifying post-therapeutic biological changes in STS, potentially enabling a more reliable assessment of tumor response to treatment.

This study aims to 1) determine the impact of the UPS treatment strategy (neoadjuvant radiotherapy with or without chemotherapy) on treatment response and 2) determine the optimal mp-MRI PWI/DCE- and CE/SWI- derived morphologic and qualitative biomarkers for assessment of response under each treatment strategy. A sub-aim is to assess the performance of these biomarkers against standard and widely used size-based criteria.

METHODS

MP-MRI protocol: All study participants underwent multiparametric MRI (MP-MRI), including diffusion-weighted imaging with apparent diffusion coefficient (DWI/ADC), contrast-enhanced susceptibility-weighted imaging (CE-SWI), and perfusion-weighted/dynamic contrast-enhanced (PWI/DCE) sequences [28, 35]. Imaging parameters were standardized to account for differences between MRI vendors and field strengths. During preoperative neoadjuvant therapy, each patient underwent multiple scans, which were consolidated into three key time points: baseline (BL, pre-therapy), post-chemotherapy (PC), and preoperative/post-radiation (PRT). For patients with soft tissue sarcoma (STS), a baseline scan was obtained for treatment-naïve tumors, followed by MRI studies during chemotherapy (ranging from one to three studies), and at least one post-radiation scan was performed one to two months after completion of radiation therapy and immediately before surgical tumor resection.

To demonstrate the clinical utility of readily available morphologic and qualitative MRI-derived features for assessing end-of-neoadjuvant therapy effect, we focused our analysis on pre-surgical (PRT) MRI. We purposefully excluded semi-quantitative, quantitative, and radiomic analyses from CE-SWI and PWI/DCE, concentrating solely on their morphologic and qualitative features. Furthermore, T2* hypointensity from treatment-induced hemorrhage can lower ADC values and mimic increased cellularity [29], potentially

leading to misleading decreases in ADC during effective therapy. Given this confounding effect and the inherently quantitative nature of ADC metrics, we excluded DWI/ADC from analysis. Instead, we centered our evaluation on the two sequences—PWI/DCE and CE-SWI—that have shown the strongest correlation with response in our prior STS response modeling research across UPS, RMS, LMS, synovial sarcoma, and desmoid tumors [24, 25, 27, 28, 29, 30, 31, 32, 34, 35].

UPS patient population

This retrospective study reviewed 5,135 MRI scans of extremity STS performed on our institution's 29-scanner fleet (1.5T and 3.0T scanners from two manufacturers) between February 2021 and March 2025. Of these, 643 UPS studies were identified, encompassing both preoperative assessments of the primary tumor and postoperative surveillance. We excluded all postoperative surveillance studies and primary UPS cases with prominent myxoid features (which exhibit higher baseline ADC values and higher T2/T2* signal due to increased water content, distinct from predominantly cellular UPS), resulting in 40 extremity cases with surgical resection. From these, the following exclusions were applied

· One without post-treatment MRI (only baseline/pre-treatment).

· Two without post-radiotherapy MRI (only post-chemotherapy).

· One without post-radiotherapy CE-SWI.

Consequently, 36 patients were included in the analysis of this study.

Surgical specimen pathology assessment

Histologic features contributing to pathologic complete response (pCR) to neoadjuvant radiotherapy, with or without chemotherapy, have been explored and may correlate with treatment outcomes. Factors evaluated included percent residual viable tumor, necrosis, hyalinization, and infarction. The presence of hyalinization or fibrosis was associated with more favorable outcomes. While these criteria have been assessed in clinical trials, they are not standard practice. In this study, all observed histologic patterns were included in the pathologic response assessment. This evaluation was performed prospectively as part of routine pathologic diagnosis and reported as estimates of percent viable tumor (or conversely, percent tumor necrosis). This determination aligns with the College of American Pathologists v4.2.0.0 sarcoma reporting elements, released in June 2024. Following our institution's standard of practice for reporting pathology treatment effects, patients were categorized into two groups based on the surgical specimen's pathology-assessed treatment effect (PATE) percentage, as described [10]. Tumors with ≥ 90% PATE were classified as responders (n = 20), while those with < 90% and > 30% were considered partial responders, and those with < 30% as non-responders. For simplicity, partial and non-responders were grouped together (n = 16).

MRI data processing

MRI datasets were transferred from imaging modalities to the institutional Picture Archiving and Communication System (IntelliSpace PACS, Philips, Amsterdam, Netherlands). MR images were retrieved from PACS, and tumors were manually contoured in three dimensions to generate segmented tumor Volumes of Interest (VOIs). VOIs were delineated and processed using multiparametric MRI (mp-MRI) with MIM software version 7.1.4 (MIM Software Inc., Cleveland, USA). This segmentation method ensured a comprehensive representation of the tumor, including areas of necrosis and enhancement. Tumor size was measured in all three orthogonal planes at each time point—baseline (BL), post-chemotherapy (PC), and pre-radiation therapy (PRT)—to estimate RECIST, WHO, and volumetric metrics. For each patient, the maximum tumor diameter (RECIST), the product of the longest and perpendicular cross-sectional diameters (WHO), and tumor volume were calculated at PC and/or PRT in comparison with BL. Based on these metrics, patients were classified as responders or partial/non-responders. Partial response threshold was set as a 30% decrease (RECIST), 50% decrease (WHO), or 50% decrease (volume), while progressive disease was indicated by a 20% (RECIST), 25% (WHO), or 25% (volume) increase, respectively [36, 37].

PWI/DCE Morphologic Patterns and Time-Intensity Curves (TICs): Following radiotherapy, PWI/DCE images stored in PACS were reviewed by an expert radiologist (over 30 years' experience) and classified into six morphologic enhancement types (Fig. 1A): capsular, unipolar, bipolar, non-nodular, semi-lunar, and solid [30, 38]. TICs from PWI/DCE imaging represent qualitative PWI/DCE characterization and generally exhibit three perfusion phases: (1) upslope, reflecting contrast wash-in; (2) plateau, indicating a steady concentration of contrast in the interstitial fluid—this may be absent in some lesions; and (3) downslope, reflecting contrast wash-out as gadolinium exits the tissue, also potentially absent in certain cases. Using a dedicated workstation (AW Server 3.2, GE HealthCare, Waukesha, WI), the radiologist assigned each TIC to one of five curve morphologies (Fig. 1B) [30, 38]. Lesions showing rapid wash-in and a brisk upstroke during the arterial phase (TIC III, IV, or V) were considered aggressive [28, 39]. Semiquantitative, quantitative, and radiomic analyses were excluded to prioritize descriptive morphologic and qualitative features accessible to practicing radiologists.

CE-SWI Morphologic Patterns: Following radiotherapy, CE-SWI images in PACS were classified by an experienced radiologist into six T2* morphologic patterns (Fig. 1C): complete ring, incomplete ring, globular, interstitial, full blooming, and no blooming. The complete ring and full blooming patterns were grouped as favorable for analysis. These morphologies have been previously reported by our group [31, 40, 41]. To determine the predominant patterns in responders versus partial/non-responders, CE-SWI morphologic patterns were compared between these groups. First- and higher-order radiomic analyses were purposefully omitted to concentrate on visually assessable morphologic features relevant to clinical practice.

Statistical Analysis

One-way chi-squared tests assessed associations between CE-SWI morphologic patterns, TIC curves, and PWI/DCE morphologic patterns and treatment response. Receiver operating characteristic (ROC)

analyses for PWI/DCE and CE-SWI patterns distinguished responders from partial or non-responders. Analyses were conducted in Python 3.10.13 using SciPy (v1.12.0) and Scikit-Learn (v1.4.1). Statistical significance was defined as $p < 0.05$.

RESULTS

Patient demographics

The study population of 36 patients ranged in age from 36 to 85 years (average 61 years). 21 were male (58%), and 15 were female (42%). A total of 23 patients received presurgical consecutive chemotherapy-radiotherapy (CT-RT), and 13 received presurgical radiotherapy (RT) alone.

Pathological Response (% of PATE)

The CT-RT group had a higher proportion of responders (n = 14, 61%) than the RT-alone group (n = 6, 46%). Consecutive CT-RT demonstrated a higher average PATE than patients receiving RT alone (81% ±25% vs. 66%±32%, P = 0.054). However, these findings were not statistically significant.

Conventional size-based response assessment metrics: Fig. 2A shows changes in longest diameter (RECIST), area (WHO), and volume in the CT-RT group with respect to baseline. In this group, most patients had stable disease per RECIST, WHO, and volume. RECIST, WHO, and volume each detected two true responses, one pseudo-response, and several true progressions and pseudo-progressions (Table 1). The changes in diameter, area, and volume in the RT alone group relative to baseline are shown in Fig. 2B. Most patients presented with RECIST, WHO, and volume stability. Only one true response was detected by volume change, and several patients presented true progression and pseudo-progression by RECIST, WHO, and volume change (Table 1).

Table 1
Number of patients that displayed true response, pseudo-response, true progression, pseudo-progression, and stability based on RECIST, WHO, and volume in the consecutive CT-RT and RT alone groups.

	Consecutive CT-RT group (n = 23)			**RT alone group (n = 13)**		
	RECIST	**WHO**	**Volume**	**RECIST**	**WHO**	**Volume**
No. of true responses	2	2	2	0	0	1
No. of pseudo-responses	1	1	1	0	0	0
No. of true progressions	1	3	1	3	4	3
No. of pseudo-progressions	1	5	4	1	2	2
No. of stable	18	12	15	9	7	7

PWI/DCE and CE-SWI morphologic and PWI/DCE qualitative (TIC) features:

In the CT-RT group (Fig. 3A), 93% of responders displayed a CE-SWI favorable (complete ring and full blooming) pattern ($P = 1.75x10^{-9}$), 86% a PWI/DCE capsular pattern ($P = 1.05x10^{-7}$), and 93% TIC type II ($P = 1.35x10^{-5}$).

In the RT group (Fig. 3B), 50% of responders displayed a CE-SWI complete ring (P = 0.225), 67% of responders displayed PWI/DCE capsular enhancement (P = 0.031), and 100% of responders displayed a TIC type II (P = 0.014).

ROC analysis and predictive response model selection

A summary of results from the ROC analysis of pathological response classification models based on PWI/DCE and CE-SWI features is presented in Fig. 4.

In patients with CT-RT (Fig. 4A), a response predictive model combining the PWI/DCE TIC type II, PWI/DCE capsular enhancement, and CE-SWI favorable (complete ring and full blooming) patterns yielded the highest classification performance (AUC = 0.996) discriminating responders vs. partial/non-responders, outperforming models based solely on capsular enhancement (AUC = 0.93), complete ring and full blooming (AUC = 0.91), TIC type II (AUC = 0.8), and RECIST (AUC = 0.52).

In patients treated with RT alone (Fig. 4B), a model based solely on TIC type II achieved perfect classification performance (AUC = 1.0), outperforming models based on capsular enhancement (AUC = 0.83), complete ring (AUC = 0.68), and RECIST (AUC = 0.5).

DISCUSSION

As a trend, the CT-RT group shows a higher proportion of responders and a higher average PATE than patients receiving RT alone; however, these differences were not statistically significant. These results are constrained by the relatively small sample size of the UPS patient population and the imbalance between the CT-RT and RT groups.

Consistent with our previous work [25, 30], our findings demonstrated that conventional size-based response assessment metrics (RECIST, WHO, and volume) were unable to distinguish responders from partial or non-responders in both CT-RT and RT groups, as most patients exhibited stable disease following NAT. Notably, the RT-alone group showed no RECIST responses and a lower incidence of pseudo-progression than the CT-RT group.

Analysis of CE-SWI and PWI/DCE morphological patterns revealed that complete-ring CE-SWI and capsular PWI/DCE patterns were more frequent in the CT-RT group, likely reflecting chemotherapy-induced tumor hemorrhage and necrosis. Observation of these patterns was less common in patients

treated with RT alone. The PWI/DCE time-intensity curve type II emerged as a distinguishing feature in responders and was present in both treatment groups, suggesting that either consecutive CT-RT or RT alone can substantially reduce tumor arterial hypervascularity, an attribute typically observed in treatment-naive and non-responding UPS.

ROC analysis identified two distinct post-treatment mp-MRI predictive response models that optimally separate responders from partial or non-responders in the CT-RT and RT-alone groups. In the CT-RT group, the best predictive model combined TIC type II, capsular enhancement, and a favorable CE-SWI pattern (complete ring or full blooming). In contrast, in the RT group, a model achieved perfect classification based solely on the presence of presurgical TIC type II. Figure 5 presents representative examples of UPS patients who responded, illustrating the defining mp-MRI features of these models. The primary distinction between the two models is the presence of hemorrhage-derived complete ring and capsular patterns of arterial enhancement, which demonstrated the strongest association with patients undergoing consecutive CT-RT.

Our previously published qualitative, semi-quantitative and first and high-order radiomic UPS mp-MRI research from 2019–2026 has demonstrated that: 1) UPS is the archetypical representation of the “cellular” STS imaging phenotype (compared to other STS with phenotypes demonstrating preponderance of myxoid, lipomatous, chondroid and fibrous components), and optimal response assessment highly correlates with imaging phenotype [24, 25]; 2) DWI/ADC has limitations in UPS response assessment due to the interference of T2* hypo-intensity due to treatment-induced hemorrhage, which lowers ADC values and mimics increased cellularity [29]; 3) hemorrhage is a clinically valuable biomarker of response, measurable with CE-SWI [31]; and 4) PWI/DCE provides valuable response information via morphological, qualitative, and semiquantitative analysis [30]. The present study further builds on the body of evidence supporting the value of UPS mp-MRI STS treatment response assessment, showing that optimal imaging biomarkers of response depend not only on tumor histology but also on the choice of treatment modality. This provides additional support for the personalized management of cancer patients.

In this study, we have introduced two novel treatment-dependent response models that predict successful treatment in UPS with PATE > 90% by solely relying on qualitative and morphological PWI/DCE and CE-SWI features. We previously reported a treatment-agnostic pre-surgical UPS response model [25] that combines the CE-SWI complete-ring, PWI/DCE capsular-enhancement, and TIC type-II (Fig. 6). Interestingly, this model was found to be the same for responding patients after consecutive CT-RT, possibly due to over-representation of this group in the cohort. The RT-alone response model was found to be much simpler, based solely on TIC type II.

Study limitations

The promising findings of this study are primarily constrained by the relatively small sample size of the UPS patient population (n = 36) and the imbalance between the CT-RT (n = 23) and RT (n = 13) groups.

The response assessment to emerging neoadjuvant immunotherapy-RT would need to be addressed separately in a future analysis.

These limitations often affect studies focusing on rare diseases such as STS. To address these limitations and strengthen the validity of our results, ongoing research involves designing and developing a prospective study to expand the current UPS cohort, likely through multi-institutional cooperation. This will enable the creation of a more balanced database of patients treated with consecutive CT-RT and RT-only regimens.

CONCLUSION

The CT-RT group demonstrated a trend toward a higher, though not statistically significant, proportion of responders and average PATE compared to RT alone. Additionally, the CT-RT responder group showed a higher rate and a significant association with morphologic features such as hemorrhage-derived CE-SWI complete-ring and necrosis-related PWI/DCE capsular patterns of arterial enhancement, likely attributable to the differential effect of added chemotherapy.

By purposefully excluding complex and clinically unavailable calculations, including semi-quantitative and quantitative PWI/DCE, first- and higher-order PWI/DCE, and CE-SWI radiomics, this study identified key mp-MRI features from PWI/DCE and CE-SWI that are readily accessible to clinical radiologists. Notably, **morphologic features** including CE-SWI “complete ring” and “full blooming,” as well as PWI/DCE “capsular enhancement” and **qualitative features** such as PWI/DCE TIC-II (with absence of rapid arterial upstroke), emerged as useful markers. These features help differentiate responders from non-responders among UPS patients treated with CT-RT or RT alone.

ROC analysis showed that in the CT-RT group, the best predictive model combined TIC type-II, capsular enhancement, and a favorable CE-SWI pattern (complete ring or full blooming), resembling previously published treatment-agnostic models. In contrast, for the RT group, a model achieved perfect classification based solely on presurgical TIC type-II. This finding suggests that optimal predictive models may vary not only by tumor type but also by treatment regimen, underscoring the importance of personalized imaging approaches.

Predictive models using these imaging features outperform RECIST in predicting pathology-assessed response and enable earlier and more accurate assessment of treatment effectiveness.

These findings add to the growing body of evidence supporting the clinical value of mp-MRI-based response models, as demonstrated by published research on UPS, leiomyosarcoma, rhabdomyosarcoma, synovial sarcoma, and desmoid tumors. Integrating mp-MRI into clinical practice may improve patient stratification, guide therapy, and advance personalized oncology.

Abbreviations

- ADC, apparent diffusion coefficient
- BL, baseline
- CE-SWI, contrast-enhanced susceptibility-weighted imaging
- DBMS, database management system
- DCE, dynamic contrast enhancement
- DWI, diffusion-weighted imaging
- Mp-MRI, multiparametric magnetic resonance imaging
- NR, non-responders
- PATE, pathology-assessed treatment effect
- PC, post-chemotherapy
- PD, progressive disease
- PR, partial responders
- PRT, post-radiation therapy
- PWI, perfusion-weighted imaging
- R, responders
- STS, soft tissue sarcoma
- SWI, susceptibility-weighted imaging
- TIF, treatment-induced fibrosis
- TIH, treatment-induced hemorrhage
- TIN, treatment-induced necrosis
- T2*, T2-star
- UPS, undifferentiated pleomorphic sarcoma
- VOI, volume of interest
- RECIST, response evaluation criteria in solid tumors

- WHO, World Health Organization

Declarations

Ethics approval and consent to participate:

- The current research article does not include animal or human experimentation and is not part of a clinical trial. All data collection, management, and processing methods were performed in accordance with the institutional and generally accepted relevant clinical, research, and ethical guidelines and regulations, including the protection of data integrity and personal health information (PHI), and in accordance with the **Declaration of Helsinki.**
- The current research was approved by the **UT MD Anderson Cancer Center Institutional Review Board (IRB)**, which waived the requirement for informed consent and approved it under **IRB identifier PA16-0857**. Protocol Name: "Utility of imaging of bone and soft tissue tumors and disease and treatment-related changes for diagnosis, prognosis, treatment response, and outcome."

Consent for publication: N.A

Availability of data and materials: The datasets used and analyzed during the current study are available from the corresponding author upon reasonable request.

Competing Interests: The authors declare not having competing private or financial interests that may conflict with the study results or design.

Funding: The ABASTI lab at MD Anderson Cancer Center in Houston received charitable funding that enabled the completion of this research from: 1) The John S. Dunn, Sr. Distinguished Chair in Diagnostic Imaging and 2) The M.R. Evelyn Hudson Foundation Endowed Professorship.

Authors' contributions: RFV, EDS, JEF, and MA participated in the data collection, segmentation, analysis, and article drafting. AF, AJL, KET, BA DMA, SL, JEM, WAM, JM, KPH, RFJ, CW, DW, NY, and CMC acted as editors and sub-topic specialists. AA, CT, PVV, and CL worked on the literature review and image curation. All authors reviewed the manuscript.

Acknowledgments: N.A

References

1. Ramakrishnan, K., et al., *Imaging of soft tissue sarcomas of the extremities with radiologic-pathologic correlation.* Current Problems in Diagnostic Radiology, 2022. **51**(6): p. 868-877.
2. Munuswamy, N., et al., *Undifferentiated Pleomorphic Sarcoma: A Case Report.* Cureus, 2024. **16**(11).
3. Makris, E.A., et al., *Natural history of undifferentiated pleomorphic sarcoma: experience from the US Sarcoma Collaborative.* Journal of surgical oncology, 2024. **129**(7): p. 1354-1363.

4. Maçaneiro, C.H., et al., *Undifferentiated pleomorphic sarcoma: prognostic factors in 42 extremity cases.* Acta ortopedica brasileira, 2023. **31**(2): p. e265942.
5. Gonzalez, M.R., et al., *Prognostic and predictive factors in undifferentiated pleomorphic sarcoma: A long-term study from a large tertiary care urban center.* J Surg Oncol, 2023. **128**(2): p. 322-331.
6. Salerno, K., et al., *Radiation therapy for treatment of soft tissue sarcoma in adults: executive summary of an ASTRO clinical practice guideline. Pract Radiat Oncol. 2021; 11 (5): 339–51*.
7. Guadagnolo, B.A., et al., *Hypofractionated, 3-week, preoperative radiotherapy for patients with soft tissue sarcomas (HYPORT-STS): a single-centre, open-label, single-arm, phase 2 trial.* The Lancet Oncology, 2022. **23**(12): p. 1547-1557.
8. Bishop, A.J., et al., *Moderately hypofractionated, preoperative radiotherapy in patients with soft tissue sarcomas (HYPORT-STS): Updated local control, late toxicities, and patient-reported outcomes.* Cancer, 2025. **131**(1): p. e35542.
9. Nathenson, M.J. and E. Sausville, *Looking for answers: the current status of neoadjuvant treatment in localized soft tissue sarcomas.* Cancer chemotherapy and pharmacology, 2016. **78**(5): p. 895-919.
10. Wardelmann, E., et al., *Evaluation of response after neoadjuvant treatment in soft tissue sarcomas; the European Organization for Research and Treatment of Cancer–Soft Tissue and Bone Sarcoma Group (EORTC–STBSG) recommendations for pathological examination and reporting.* European journal of cancer, 2016. **53**: p. 84-95.
11. Soldatos, T., et al., *Multiparametric assessment of treatment response in high-grade soft-tissue sarcomas with anatomic and functional MR imaging sequences.* Radiology, 2016. **278**(3): p. 831-840.
12. Boulouta, A., et al., *Pathologic complete response in patients with localized soft tissue sarcoma treated with neoadjuvant therapy and its correlation with clinical outcomes: A systematic review.* Cancer Treatment Reviews, 2024. **130**: p. 102820.
13. Eilber, F.C., et al., *Treatment-induced pathologic necrosis: a predictor of local recurrence and survival in patients receiving neoadjuvant therapy for high-grade extremity soft tissue sarcomas.* Journal of clinical oncology, 2001. **19**(13): p. 3203-3209.
14. Salah, S., et al., *Tumor necrosis and clinical outcomes following neoadjuvant therapy in soft tissue sarcoma: A systematic review and meta-analysis.* Cancer treatment reviews, 2018. **69**: p. 1-10.
15. Bonvalot, S., et al., *Complete pathological response to neoadjuvant treatment is associated with better survival outcomes in patients with soft tissue sarcoma: Results of a retrospective multicenter study.* European Journal of Surgical Oncology, 2021. **47**(8): p. 2166-2172.
16. Donahue, T.R., et al., *Evaluation of neoadjuvant therapy and histopathologic response in primary, high-grade retroperitoneal sarcomas using the sarcoma nomogram.* Cancer, 2010. **116**(16): p. 3883-3891.
17. Wang, D., et al., *Pathologic complete response and clinical outcomes in patients with localized soft tissue sarcoma treated with neoadjuvant chemoradiotherapy or radiotherapy: the NRG/RTOG 9514 and 0630 nonrandomized clinical trials.* JAMA oncology, 2023. **9**(5): p. 646-655.
18. Gennaro, N., et al., *Heterogeneity in response to neoadjuvant radiotherapy between soft tissue sarcoma histotypes: Associations between radiology and pathology findings.* European Radiology,

2025. **35**(3): p. 1337-1350.

19. Renn, A., et al., *Overview of malignant soft-tissue sarcomas of the limbs.* Clinical Radiology, 2021. **76**(12): p. 940. e1-940. e16.
20. Reddy, R., *Primary undifferentiated pleomorphic sarcoma of the biceps femoris muscle complicated by hemorrhage: an underrecognized entity.* Cureus, 2021. **13**(8).
21. Koh, D.-M. and D.J. Collins, *Diffusion-weighted MRI in the body: applications and challenges in oncology.* American Journal of Roentgenology, 2007. **188**(6): p. 1622-1635.
22. Jahng, G.-H., et al., *Perfusion magnetic resonance imaging: a comprehensive update on principles and techniques.* Korean journal of radiology, 2014. **15**(5): p. 554-577.
23. Haller, S., et al., *Susceptibility-weighted imaging: technical essentials and clinical neurologic applications.* Radiology, 2021. **299**(1): p. 3-26.
24. Valenzuela, R., et al., *Multiparametric MRI for the assessment of treatment effect and tumor recurrence in soft-tissue sarcoma of the extremities.* J. Radiol. Oncol, 2023. **7**(3): p. 058-065.
25. Valenzuela, R.F., et al., *Building a pre-surgical multiparametric-MRI-based morphologic, qualitative, semiquantitative, first and high-order radiomic predictive treatment response model for undifferentiated pleomorphic sarcoma to replace RECIST.* Cancer Imaging, 2025. **25**(1): p. 56.
26. Eisenhauer, E.A., et al., *New response evaluation criteria in solid tumours: revised RECIST guideline (version 1.1).* European journal of cancer, 2009. **45**(2): p. 228-247.
27. Raul Fernando Valenzuela, J.E.M., Vikas Kundra, Colleen M. Costelloe, *Advanced Imaging in Musculoskeletal Oncology: Moving Away From RECIST and Embracing Advanced Bone and Soft Tissue Tumor Imaging (ABASTI)—Part II—Novel Functional Imaging Techniques.* Seminars in Ultrasound, CT and MRI, 2021. **42**(2): p. 215-227.
28. Valenzuela, R.F., et al. *Advanced Imaging in Musculoskeletal Oncology: Moving Away From RECIST and Embracing Advanced Bone and Soft Tissue Tumor Imaging (ABASTI)-Part I-Tumor Response Criteria and Established Functional Imaging Techniques*. in *Seminars in Ultrasound, CT and MRI*. 2021. Elsevier.
29. Valenzuela, R., et al., *Radiomics by Quantitative Diffusion-weighted MRI for Predicting Response in Patients with Extremity Soft-tissue Undifferentiated Pleomorphic Sarcoma.* Journal of Radiology and Oncology, 2024. **8**(2): p. 064-071.
30. Valenzuela, R., et al., *Perfusion-weighted imaging with dynamic contrast enhancement (PWI/DCE) morphologic, qualitative, semiquantitative, and radiomics features predicting undifferentiated pleomorphic sarcoma (UPS) treatment response.* Scientific Reports, 2024. **14**(1): p. 21681.
31. Valenzuela, R.F., et al., *Novel Use and Value of Contrast-Enhanced Susceptibility-Weighted Imaging Morphologic and Radiomic Features in Predicting Extremity Soft Tissue Undifferentiated Pleomorphic Sarcoma Treatment Response.* JCO Clinical Cancer Informatics, 2025. **9**: p. e2400042.
32. B. Amini, E.D.-S., J. Madewell, W. Murphy, C. Costelloe, R. F. Valenzuela, *Advanced MRI can be used to determine percent necrosis in leiomyosarcoma.* ECR 2024, 2024.

33. Valenzuela, R.F., et al., *A follow-up study on the novel use of contrast-enhanced susceptibility-weighted imaging for extremity desmoid fibromatosis response assessment.* Scientific Reports, 2025. **15**(1): p. 20515.
34. Valenzuela, R.F., et al., *Early results in the novel use of contrast-enhanced susceptibility-weighted imaging in the assessment of response and progression in desmoid fibromatosis: A pilot study in a specialized cancer institution.* Tumor Discovery, 2023. **2**(3): p. 1414.
35. Valenzuela, R.F., et al., *Multiparametric MRI for the Assessment of Treatment Effect and Tumor Recurrence in Soft-tissue Sarcoma of the Extremities.* Journal of Radiology and Oncology, 2023. **7**(3): p. 058-065.
36. Subhawong, T.K., et al., *MRI volumetrics and image texture analysis in assessing systemic treatment response in extra-abdominal desmoid fibromatosis.* Radiology: Imaging Cancer, 2021. **3**(4): p. e210016.
37. Shah, G.D., et al., *Comparison of linear and volumetric criteria in assessing tumor response in adult high-grade gliomas.* Neuro-oncology, 2006. **8**(1): p. 38-46.
38. R. F. Valenzuela, E.D.-S., M. Canjirathinkal, C. Costelloe, H. Idrees, J. Madewell, W. Murphy, B. Amini, *Perfusion weighted imaging with dynamic contrast enhancement (PWI/DCE) for the treatment assessment of extremity soft-tissue non-myxoid undifferentiated pleomorphic sarcoma.* European Congress of Radiology 2024, 2024.
39. Subhawong, T.K. and B.A. Wilky, *Value added: functional MR imaging in management of bone and soft tissue sarcomas.* Current opinion in oncology, 2015. **27**(4): p. 323-331.
40. R. F. Valenzuela, B.A., E. Duran-Sierra, M. Canjirathinkal, H. Idrees, J. Madewell, C. Costelloe, W. Murphy, *Susceptibility-Weighted Imaging (SWI) in Benign and Malignant Tumors of the Musculoskeletal System.* European Congress of Radiology 2023, 2023.
41. E. Duran-Sierra, R.F.V., M. Canjirathinkal, J. Madewell, W. Murphy, C. Costelloe, B. Amini, *Susceptibility Imaging (SWI) Morphologic Patterns and High-Order Radiomics of Baseline and Post-Treatment Advanced MRI of Extremity Soft-Tissue Undifferentiated Pleomorphic Sarcoma.* European Congress of Radiology 2023, 2023.

Figures

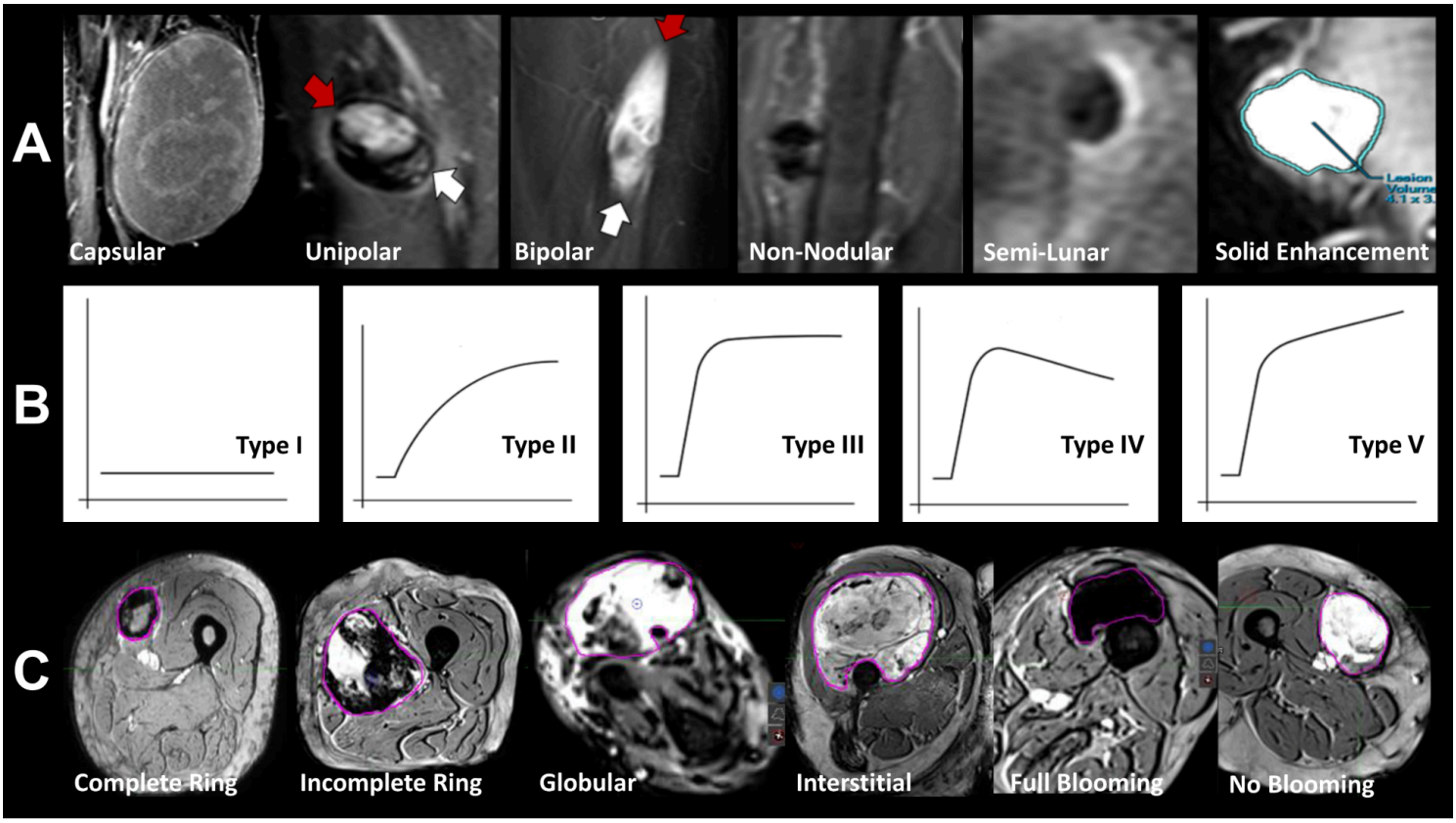


Figure 1

Representative imaging patterns of UPS categorized by an experienced radiologist. (A) Six PWI/DCE morphologic patterns, (B) Five qualitative PWI/DCE time-intensity curve types, and (C) Six CE-SWI morphologic patterns. Figure modified with permission from R.F. Valenzuela et al. [25].

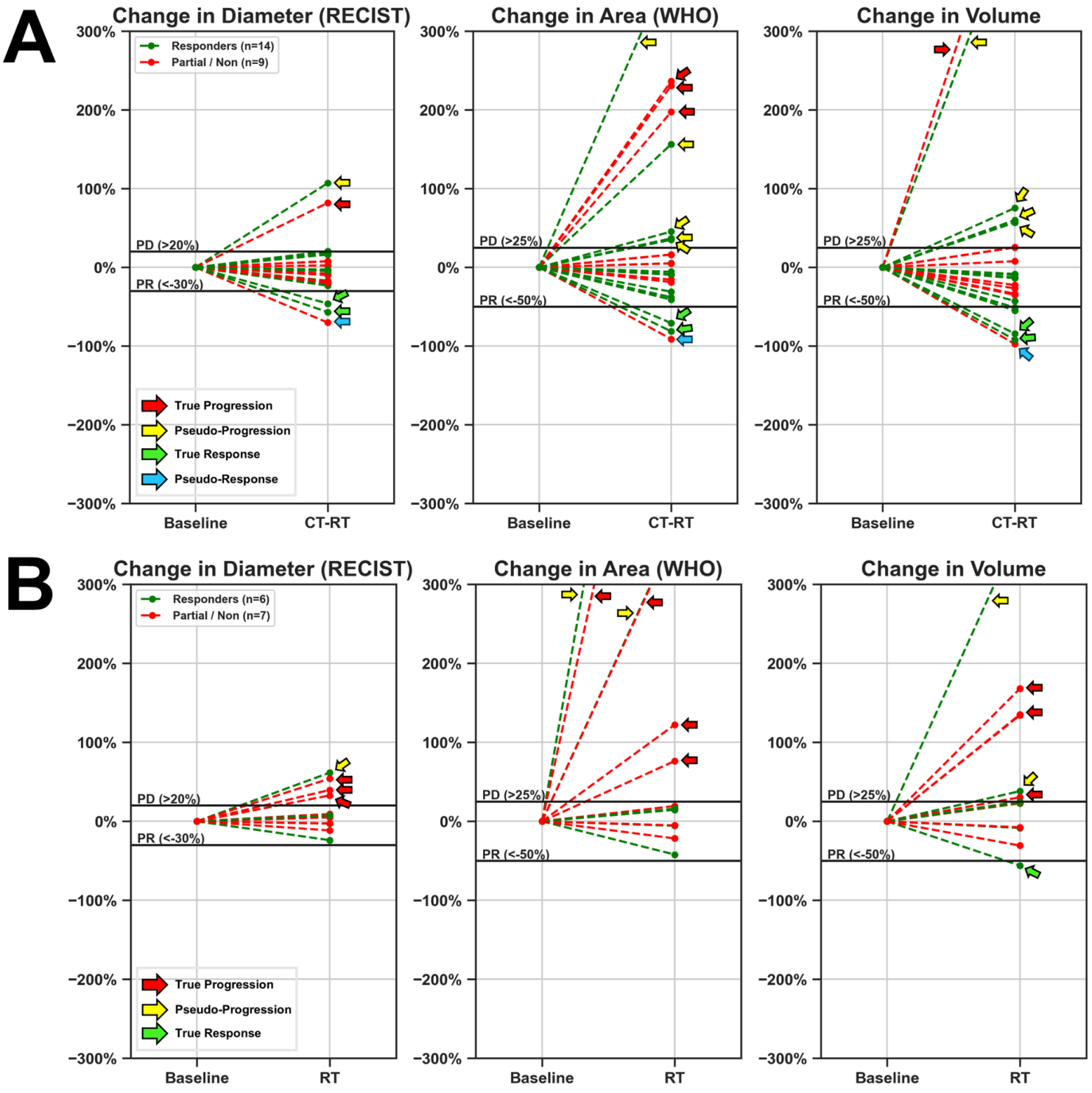


Figure 2

Conventional size-based response assessment of metrics in (A) the consecutive CT-RT group and (B) the RT alone group. Most patients had stable disease by RECIST, WHO, and volume criteria. Thresholds for partial response (PR) and progressive disease (PD) are indicated by solid horizontal lines. In the CT-RT group, two responses and one pseudo-response were detected by RECIST, WHO, and volume. In the RT group, volume detected one response that RECIST or WHO did not.

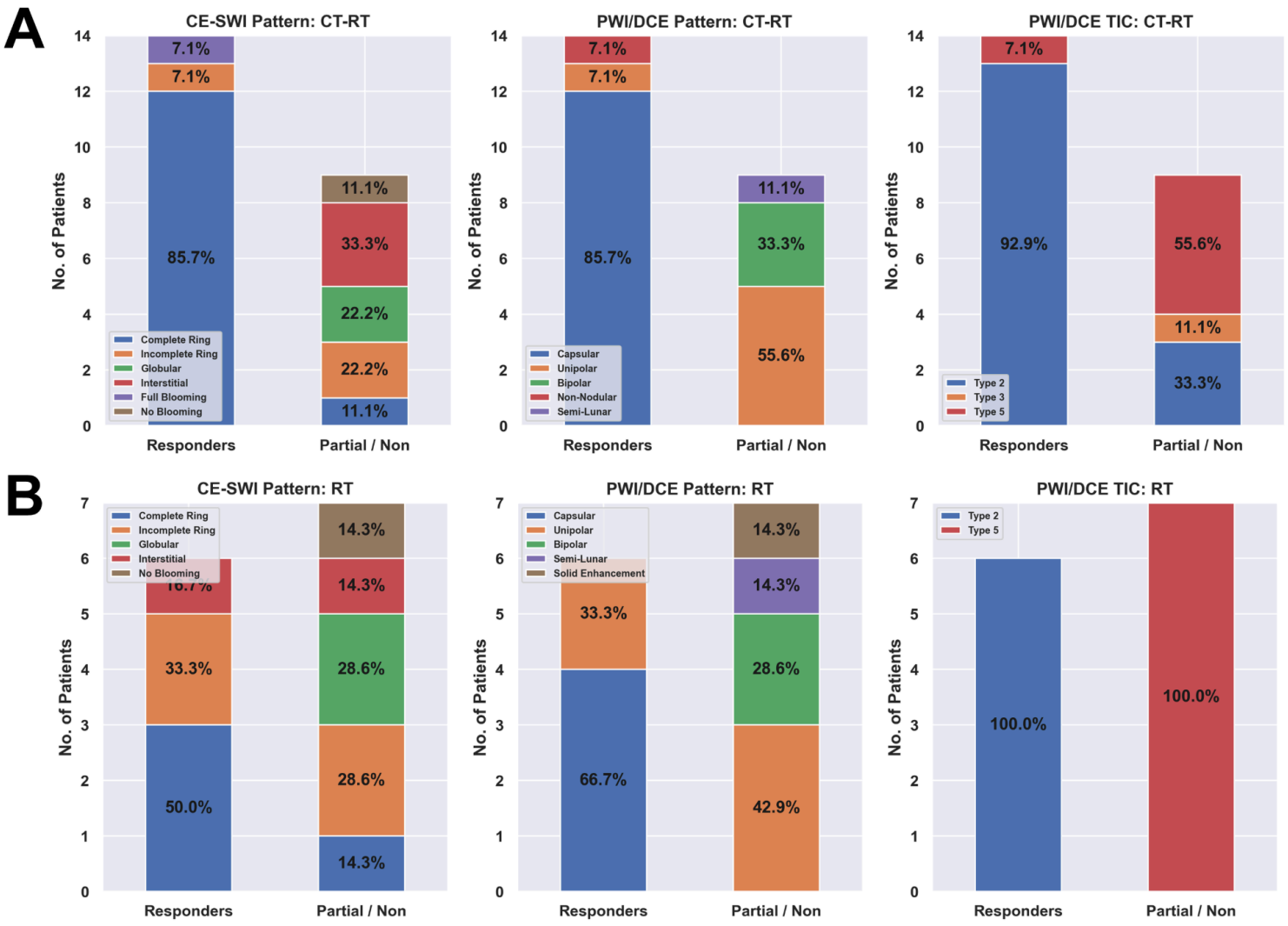


Figure 3

CE-SWI and PWI/DCE patterns observed in (A) the consecutive CT-RT group and (B) the RT alone group. CT-RT responders displayed high statistical associations with the CE-SWI favorable (complete ring and full blooming) patterns ($P=1.75x10^{-9}$), PWI/DCE capsular enhancement ($P=1.05x10^{-7}$), and TIC type II ($P=1.35x10^{-5}$). Among RT responders, the complete ring ($P=0.225$) and capsular ($P=0.031$) patterns were less frequently observed, whereas TIC type II was present in all of them ($P=0.014$).

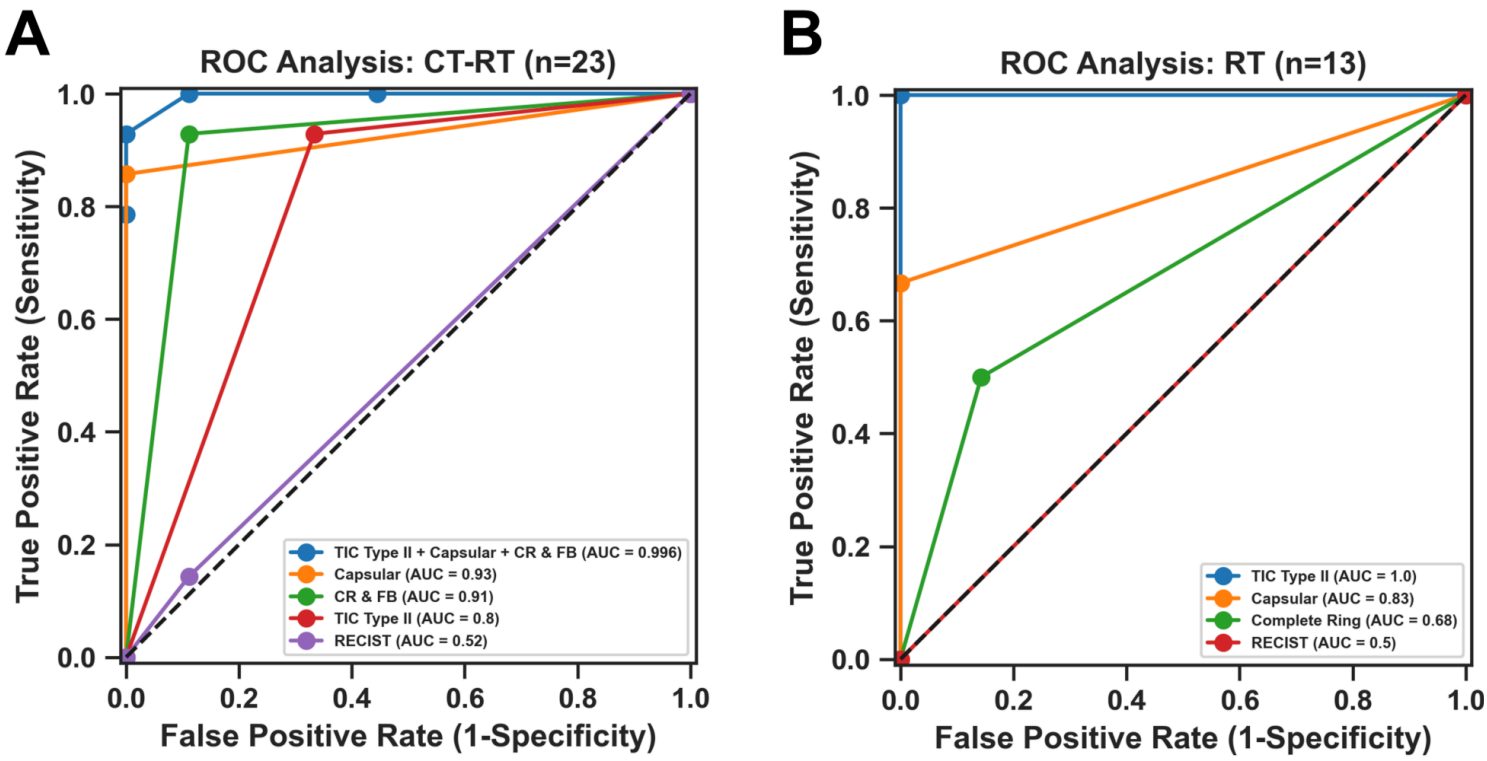


Figure 4

Summary of ROC analysis of classification models based on CE-SWI and PWI/DCE features discriminating responders from partial/non-responders. In the CT-RT group (A), the best-performing model (AUC=0.996) combined PWI/DCE TIC type II and capsular enhancement, and CE-SWI complete-ring and full-blooming patterns, whereas in the RT group (B), the model based solely on TIC type II achieved perfect performance (AUC=1.0). In both groups, these models significantly outperformed RECIST. Note: On panel B, RECIST overlaps the diagonal line (representing a random classifier). CR: Complete Ring; FB: Full Blooming.

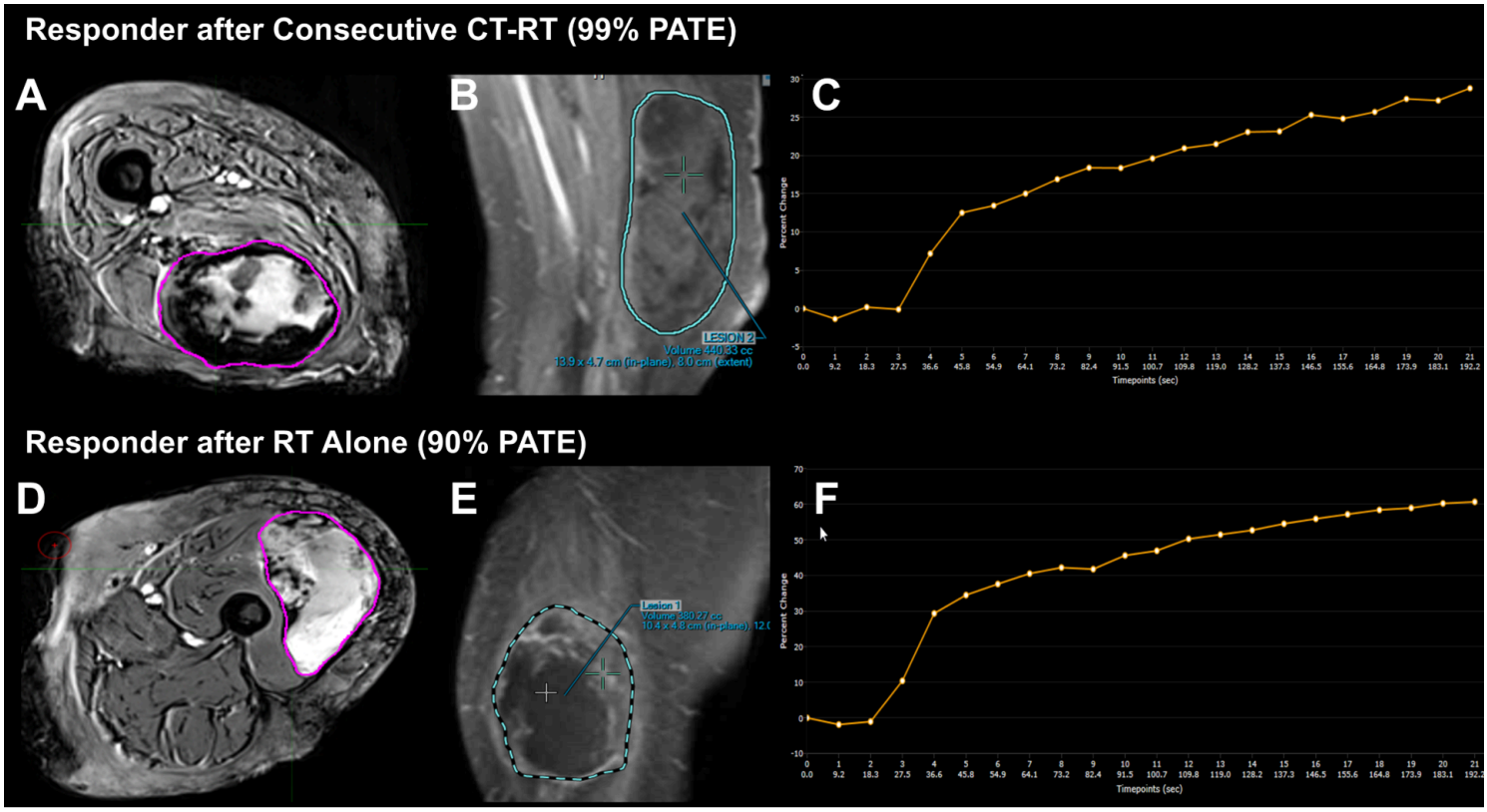


Figure 5

Top panels: Representative responder after consecutive CT-RT showing (A) CE-SWI Complete Ring, (B) PWI/DCE Capsular enhancement, and (C) PWI/DCE TIC type II. Bottom panels: Representative responder after RT alone showing (D) CE-SWI Incomplete Ring, (E) PWI/DCE Unipolar enhancement, and (F) PWI/DCE TIC type II.

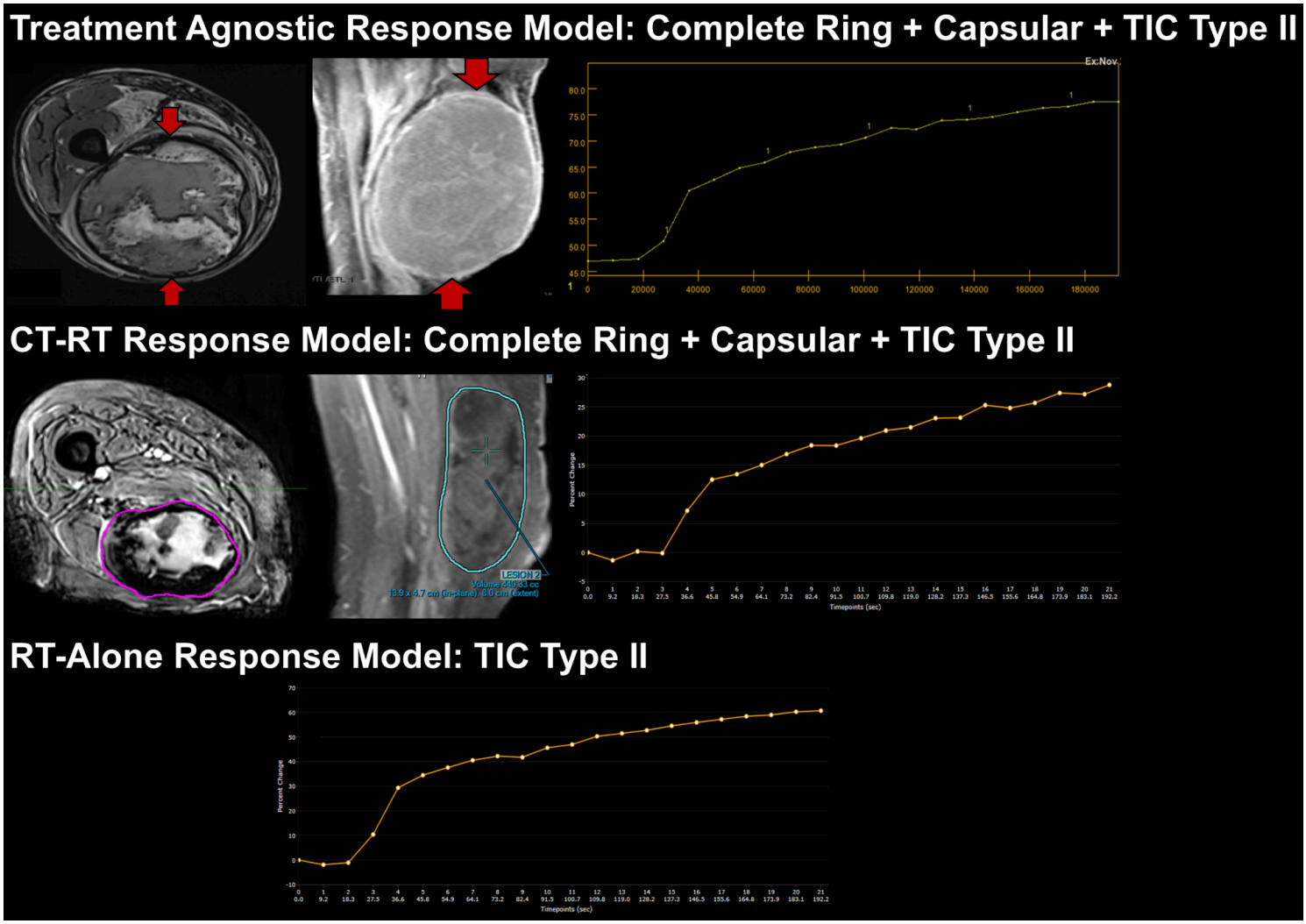


Figure 6

Representative examples of CE-SWI and PWI/DCE features that define the optimal treatment-specific UPS response models. The treatment-agnostic response model, previously reported by our group, combines the complete ring, capsular enhancement, and TIC type II, and was found to be the same in responding patients after consecutive CT-RT. The RT-alone response model was based solely on the TIC type II.